

# Markarian 421's Unusual Satellite Galaxy

P. W. Gorham <sup>1</sup>, L. van Zee <sup>2</sup> S. C. Unwin <sup>1</sup>, and C. S. Jacobs <sup>1</sup>

1. Jet Propulsion Laboratory,  
Pasadena, California, 91109

2. National Radio Astronomical Observatory,  
PO Box 0, Socorro, New Mexico

## ABSTRACT

We present Hubble Space Telescope (HST) imagery, and ground-based spectroscopy and CCD photometry of the active galaxy Markarian 421 and its companion galaxy 14 arcsec to the ENE. The HST images indicate that the companion is a morphological spiral rather than elliptical as previous ground-based imaging has concluded. The companion has a bright, compact nucleus, appearing unresolved in the HST images. This is suggestive of Seyfert activity, or possibly a highly luminous compact star cluster. Ground-based CCD photometry of the nucleus of the companion galaxy indicates that its color is distinct from its surrounding bulge, strengthening the identification of nuclear activity.

We also report the results of high dynamic range long-slit spectroscopy with the slit placed to extend across both galaxies and nuclei. We detect no emission lines in the companion nucleus, though there is evidence for recent star formation. Velocities derived from a number of absorption lines visible in both galaxies indicate that the two systems are probably tidally bound and thus in close physical proximity. Using the measured relative velocities, we derive a lower limit on the MKN 421 mass within the companion orbit ( $R \sim 10$  kpc) of  $5.9 \times 10^{11}$  solar masses, and a mass-to-light ratio of  $\geq 17$ .

Our spectroscopy also shows for the first time the presence of  $H\alpha$  and [NII] emission lines from the nucleus of MKN 421, providing another example of the appearance of new emission features in the previously featureless spectrum of a classical BL Lac object. We see both broad and narrow line emission, with a velocity dispersion of several thousand  $\text{km s}^{-1}$  evident in the broad lines. Based on the imagery and broad-line velocity dispersion we find evidence for a black hole with mass of order  $10^9 M_{\odot}$  at the center of MKN 421.

*Subject headings:* galaxies: BL lacertae objects: individual (Markarian 421) — galaxies: binary — galaxies: interactions

## 1. Introduction

Markarian 421 is a giant elliptical galaxy that contains the nearest BL Lac object, at a redshift of 0.031 (Ulrich et al. 1975). This object is among the most intensively studied of all active galactic nuclei (AGN). MKN 421 is a strong cm-wavelength radio source that has shown reported superluminal motion in its compact radio jet (Zhang and Baath 1990), although recent measurements (Piner et al. 1999) do not confirm this. It is optically highly variable in both intensity and polarization. It is seen in X-rays (Comastri et al. 1997), GeV gamma-rays (Mukherjee et al. 1997), and up to multi-TeV energies (Krennrich et al. 1997). Episodes of rapid variability have been seen repeatedly at many wavelengths (Tosti et al. 1998; Gaidos et al. 1996) strengthening the evidence for the presence of a compact object as the source of the nuclear activity.

The host galaxy of MKN 421 has been the subject of several spectroscopic and photometric studies. The first such study (Ulrich 1975) established the redshift ( $z=0.0308$ ) based on weak stellar absorption lines, and also noted that a nearby galaxy 14 arcsec to the ENE had a similar redshift ( $z=0.0316$ ), indicating that it was probably physically related, although if the velocity difference were due to the Hubble flow, the distance could be a few Mpc or more. The companion galaxy was classified as a normal elliptical (Hickson et al. 1984). Further work by Ulrich (1978) showed that MKN 421 was the brightest member of a group of 5–7 galaxies of similar redshift spread over a region of sky of order 10 arcmin in radius. The presence of this group increases the likelihood that the companion’s proximity to MKN 421 is physical rather than a random alignment.

There is mounting evidence that AGN phenomena appear to be associated with galaxy mergers or encounters (cf. Shlosman, Begelman, and Frank 1990; Hernquist & Mihos 1995). In the case of BL Lac objects, a significant number have been found in the last decade or so to be associated with close companions or groups of nearby galaxies (cf. Falomo 1996; Heidt 1999), although MKN 421 has apparently been overlooked in this regard. Thus intrigued by the proximity of these two galaxies, we have acquired and analyzed previously unpublished HST imagery of the system, and performed Palomar 1.5 m photometric and Hale 5 m long-slit spectroscopic observations aimed at clarifying this association.

Our goal was to understand the nature of the nearby galaxy in relation to MKN 421, and to investigate the properties of the companion galaxy itself. If the galaxy is as close to MKN 421 as its projected distance ( $\sim 10$  Kpc) suggests, it is deep within the gravitational potential well of MKN 421, and is probably sweeping through its stellar halo. The conditions under which such an encounter can take place are of general interest in the understanding of galaxy evolution. Our results will show that the companion galaxy contains a Seyfert-like nucleus, and is likely to be tidally interacting with MKN 421. Although the evidence is circumstantial, this association does appear to lend weight to the suggestions that galaxy encounters are an important factor in AGN evolution, and that close companions are associated in some way with the BL Lac phenomenon.

In the following section we summarize the the imagery and photometry which indicate nuclear activity in the companion galaxy. Section 3 summarizes the spectroscopic results, from which we derive a velocity profile which indicates a system that is tidally bound. Section 4 presents some further analysis of the spectroscopic results, including a derived lower limit of the bulge mass and mass-to-light ratio of MKN 421 under some plausible assumptions. Section 5 summarizes and concludes the article.

## 2. Observations

A complete log of all observations presented here is shown in Table 1. The following sections discuss each of the observations in the same order as shown in the table.

In the work of Ulrich (1978), the system  $14''$  to the ENE of MKN 421 was denoted as galaxy number 5 of the group of galaxies associated with MKN 421. Although the galaxy had been noticed prior to this work, it appears that Ulrich was the first to provide a designation for it. Thus we will refer to it in this present work as MKN 421-5.

We note that users of NASA’s Extragalactic Database (NED) may find a reference to this object as RX J1104.4+3812:[BEV98] 014. However, since this reference is only used to distinguish objects within the ROSAT error circle for MKN 421, and the object is previously known, we prefer the designation given by Ulrich (1978).

### 2.1. Imagery and Photometry

#### 2.1.1. *HST* images & photometry

MKN 421 was observed with the HST wide field/planetary camera (WF/PC2) on 1997 March 05, using the F702W filter. Five exposures, one of duration 2 s, two of duration 30 s, and two of duration 120 s were made <sup>1</sup>. The images were prepared by standard techniques described in Holtzman et al. (1995), and the moderate cosmic ray contamination of the frames was repaired by hand using linear interpolation. In the 2 s exposure, the MKN 421 nucleus is not saturated, but the companion galaxy is underexposed. The remaining two images overexpose the AGN, but for both MKN 421’s host galaxy and the companion galaxy the exposures provide good signal-to-noise ratios over the sky background. The pixel scale in these images is 0.0455 arcsec per pixel, and the resolution of HST at the mean filter wavelength (690 nm) is  $\sim 0.080$  arcsec; thus the images are sampled just slightly under the Nyquist frequency.

---

<sup>1</sup>The HST observations used here are available as part of the STSCI public archive, and were made originally as a result of a proposal by C. M. Urry.

Secondary corrections, including those associated with the known gradient in charge transfer efficiency and the pixel area variation across the frame (Holtzman et al. 1995), are not corrected for in the displayed images, but we have applied first-order corrections for these effects in the relative photometry presented in the next section.

Figure 1 shows a slightly smoothed grayscale of the summed image, with a logarithmic stretch and quantized levels chosen to show the details of the host galaxy of MKN 421 and MKN 421-5. Several features of MK421-5 are evident even from this image. First, its structure is not a simple elliptical. A suggestion of spiral arms is evident, and possible evidence of barlike structure appears at the outer edges of the galaxy. Second, the nucleus of the companion is clearly brightened relative to the galactic bulge, as is shown in the inset frame. Third, there is no evidence for any obvious dust lanes or similar absorption features in either the outer or bulge regions of the galaxy.

Figures 2–4 illustrate these features. In Figure 2 we show more quantitative evidence for the presence of spiral structure, since the structure is difficult to reproduce adequately in paper copies of the images themselves. Fig. 2(a) is a grayscale plot centered on the companion galaxy, including overlaid contours which emphasize the disk regions, showing structure which is suggestive of spiral arms. In Fig. 2(b) we show centroids of the surface brightness distributions in slices along the galaxy major axis in Fig. 2(a). The displacement of the brightness centroids clearly shows the presence of spiral structure. (The amplitude of the centroid displacement does not directly track the location of the arms, since it depends on the brightness of the arm structure relative to the surrounding disk.)

In Figures 3 and 4 we show a single row slice through the AGN and the companion, both plotted on linear scales. Given the HST frame orientation, this is nearly an east–west slice, and is roughly parallel to the galaxy major axis. The companion nucleus appears about 2 mag brighter than the surrounding bulge, and appears nearly unresolved in this image. At a distance of 130 Mpc (for  $h = 0.65$ ), a single HST pixel corresponds to about 33 pc. Thus the bright nucleus appears too compact to be a typical star forming region. As we discuss in a later section, it is likely to be either a compact nuclear star cluster or more probably an active nucleus.

In Table 2, we give results of F702W filter photometry using the HST images. The F702W filter is roughly coincident with a Cousins R filter, although it is somewhat wider and slightly shifted toward the red. The magnitudes given in Table 2 show MKN 421 to be somewhat brighter than typical ground-based photometric values. We have also converted the measured magnitudes to absolute magnitudes using  $h = 0.65$ , for use in later discussion.

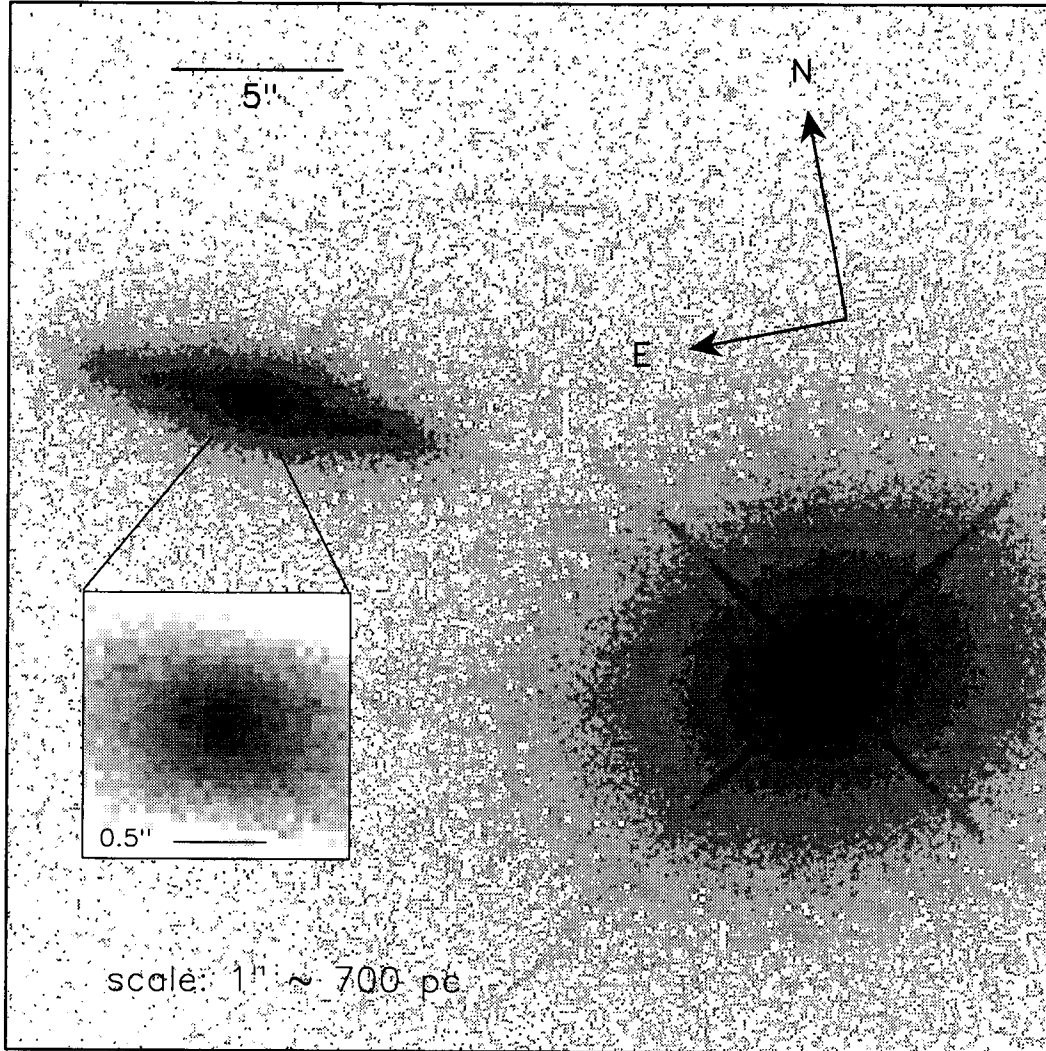


Fig. 1.— HST image of MKN 421 and companion MKN 421-5, through red F702W filter, 300 s total exposure. In the larger image the cores of MKN 421 and the companion are saturated to show detail of the companion disk structure. Levels are quantized to more clearly show the companion structure. The inset shows the nucleus of the companion plotted with a logarithmic stretch, showing the bright, unresolved nucleus. The scale in is approximately 700 pc/arcsec for  $h = 0.65$

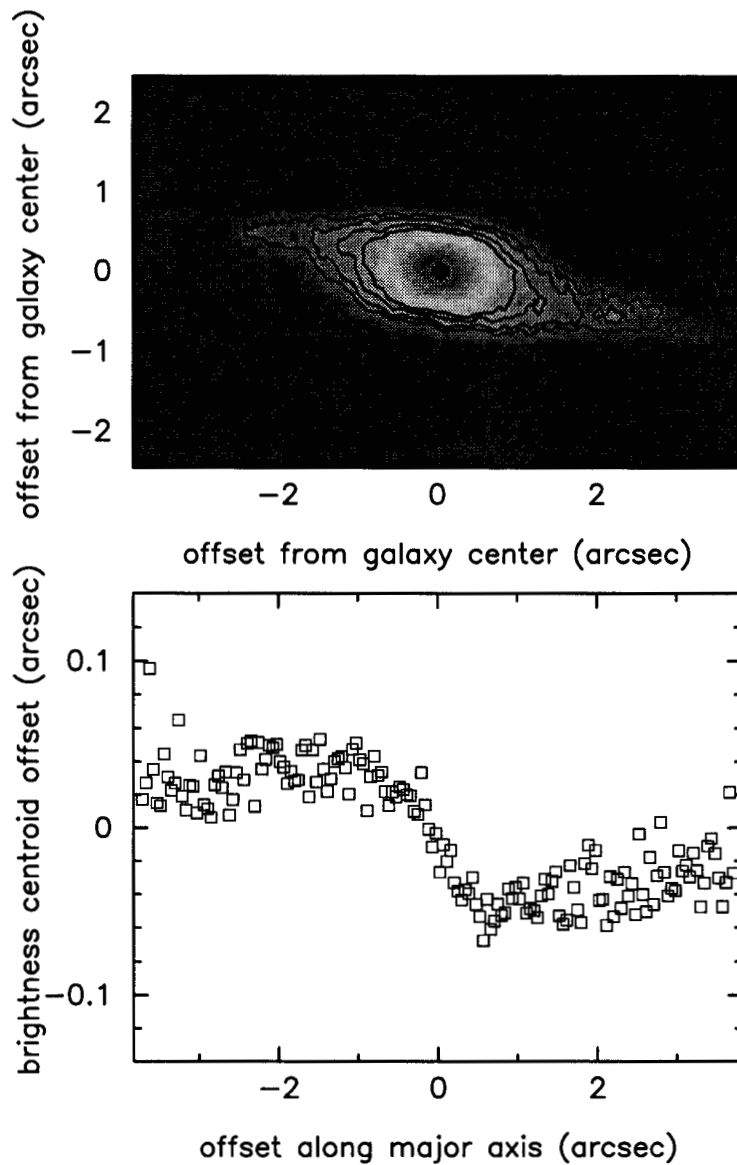


Fig. 2.— (a) Logarithmic grayscale of a smoothed HST image of MKN 421-5. Central portions saturated to show disk more clearly. (b) Plot of surface brightness centroids of slices perpendicular to the major axis showing evidence of spiral structure.

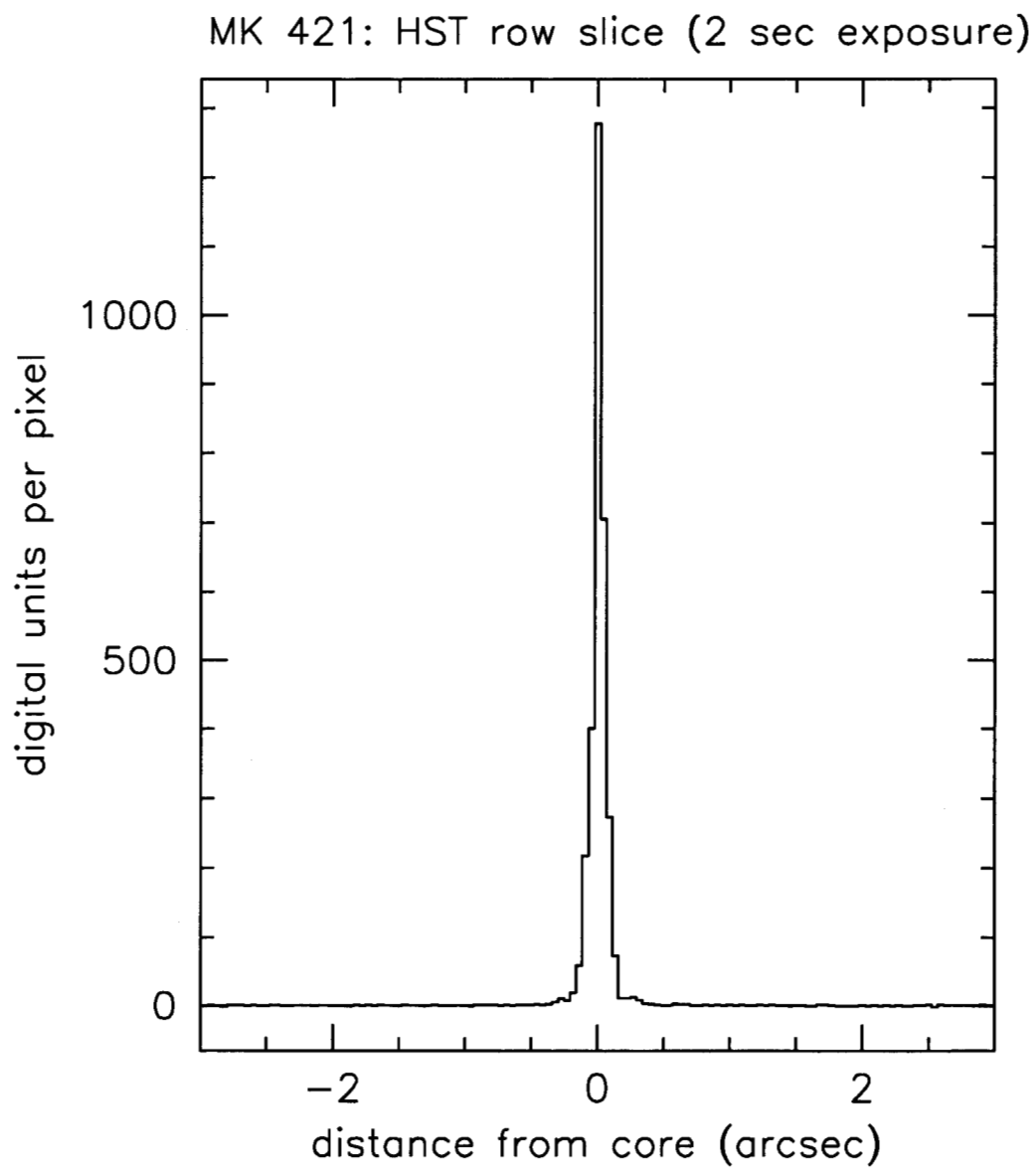


Fig. 3.— A single column slice through a 2 sec exposure HST R-band image of MKN 421's nucleus, showing the HST point spread function.

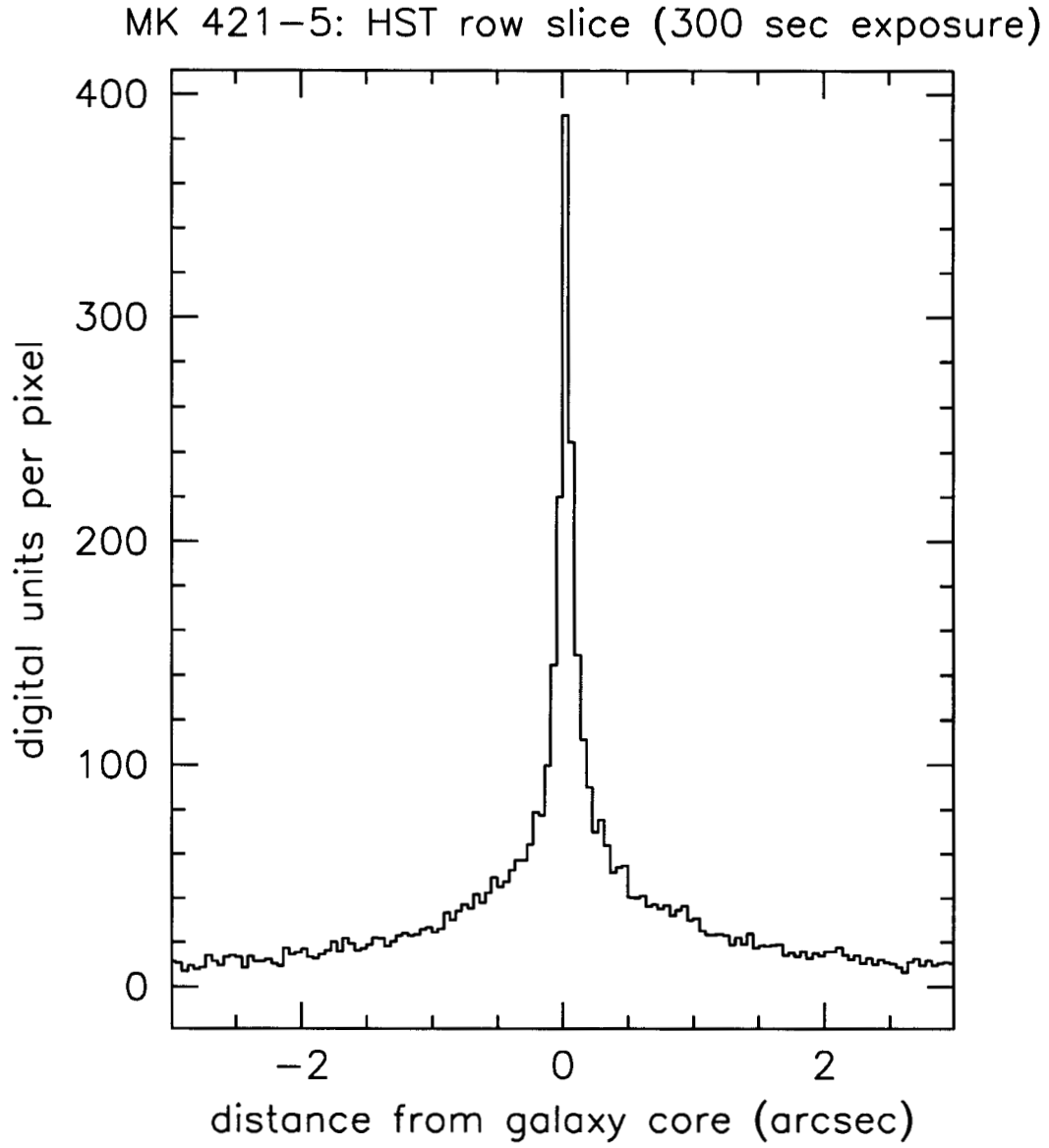


Fig. 4.— A single column slice through the companion galaxy nucleus, showing a compact nucleus surrounded by a centrally brightened bulge region. This image has a 300 sec total exposure.



### 2.1.2. Palomar CCD Photometry

We obtained CCD images of MKN 421 and its companion during the night of 1999 February 19 using the Palomar Observatory 1.5 m telescope, using Gunn  $r, i$  filters<sup>2</sup>. The night was not photometric, but seeing was moderately good (1-1.5 arcsec) and relatively stable during the observations. The absolute accuracy of the magnitudes is reliable only to 0.1 mag, but the relative colors should be still quite accurate. The magnitude calibration is based on the observation of standard stars during the night, taken from Landolt (1992).

Table 3 shows the results of the Palomar photometry, with statistical errors (not including the overall calibration uncertainty mentioned above) given for each measurement. The magnitudes have been transformed to Cousins  $R, I$  magnitudes according to the transformations given in Wade et al. (1979). MKN 421 is at a galactic latitude of  $b = 65^\circ$  so reddening corrections for  $R$  and  $I$  are negligible. as are the redshift corrections given by Sandage (1976).

It is evident from the photometry that the nucleus of MKN 421-5 appears to be rising in the red somewhat faster than the surrounding bulge. This behavior is typical of Seyfert 2 nuclei. Clearly further photometry in the near infrared would shed more light on this issue.

MKN 421 is highly variable in the visual bands. In fact, the HST observations in early 1997 occurred just after a large optical outburst (Tosti et al. 1998) during which the  $R$ -band magnitude peaked at brighter than 12. During March 1997, Tosti et al. estimated  $R = 12.4$  from ground-based photometry. Although this is about 0.9 mag fainter than the HST estimate, the difference can be accounted for by dilution effects convolved with the differing AGN and host galaxy spectral energy distributions and the effects of seeing and atmospheric absorption. Similar effects can also account for the fainter estimated magnitude of the companion nucleus in the HST image as compared to the ground-based images.

## 3. Optical Spectroscopy

Low resolution optical spectra of MKN 421 and its companion were obtained with the Double Spectrograph on the 5m Palomar<sup>3</sup> telescope during the night of 1999 February 19. The long slit (2') with a 2'' aperture was centered on the companion galaxy and two 600 sec exposures were obtained. The slit was positioned at an angle of  $53^\circ$ , and passed through both the companion galaxy and the nucleus of MKN 421. A 5500 Å dichroic was used to split the light to the two sides (blue and red), providing complete spectral coverage from 3600–7600 Å. The blue spectra

---

<sup>2</sup>These observations at the Palomar Observatory were made as part of a continuing cooperative agreement between the Jet Propulsion Laboratory and the California Institute of Technology.

<sup>3</sup>These observations at the Palomar Observatory were made as part of a continuing cooperative agreement between Cornell University and the California Institute of Technology.

Table 1: Log of observations presented here.

Date	Telescope	Instrument	Filter/grating
1997 March 5	HST	WF/PC2	F702W
1999 February 17	Palomar 1.5m	CCD4	Gunn r,i
1999 February 19	Palomar 1.5m	CCD13	Gunn r,i
1999 February 19	Palomar 5m	Double Spect.	600/300 l/mm

Table 2: HST F702W filter photometry of MKN 421 & companion.

Source	$m_{702w}$	$M_{702w}$	units
MKN 421 AGN	$11.48 \pm 0.10$	-24.22	mag
MKN 421-5 nucleus	$18.78 \pm 0.12$	-16.92	mag

Table 3: Palomar 1.5m CCD Photometry on MKN 421 & companion.

Source	$R$	$I$	$(R - I)$	units
MKN 421 AGN	$13.27 \pm 0.03$	$13.00 \pm 0.04$	$0.27 \pm 0.05$	mag
MKN 421-5 nucleus	$17.16 \pm 0.03$	$16.82 \pm 0.03$	$0.34 \pm 0.04$	mag
MKN 421-5 bulge	$17.92 \pm 0.03$	$17.78 \pm 0.03$	$0.15 \pm 0.04$	mag arcsec <sup>-2</sup>

were acquired with the 600 lines/mm diffraction grating (blazed at 4000 Å). The red spectra were acquired with the 316 lines/mm diffraction grating (blazed at 7500 Å). Thinned 1024×1024 Tek CCDs, with read noises of 8.6 e<sup>-</sup> (blue) and 7.5 e<sup>-</sup> (red), were used on the two sides of the spectrograph. Both CCDs had a gain of 2. e<sup>-</sup>/(digital unit). The effective spectral resolution of the blue camera was 5.0 Å (1.72 Å/pix); the effective spectral resolution of the red camera was 7.9 Å (2.47 Å/pix). The spatial scale of the long slit was 0.62 "/pix for the blue camera and 0.48 "/pix for the red camera.

The spectra were reduced and analyzed with the IRAF<sup>4</sup> package. The spectral reduction included bias subtraction, scattered light corrections, and flat fielding with both twilight and dome flats. The 2-dimensional images were rectified based on arc lamp observations (Fe and Ar for the blue side; He, Ne, and Ar for the red side) and the trace of stars at different positions along the slit. The sky background was removed from the 2-dimensional images by fitting a low order polynomial along each row of the spectra. One dimensional spectra of MKN 421 and its companion were extracted from the rectified images using a 1.5" extraction region (the seeing disk at the time of the observations) centered on the peak emission of each system. In addition, a galaxy spectrum for MKN 421 was obtained by averaging together two 4" regions offset from the nucleus by ±4". While the night was non-photometric, observations of standard stars from the list of Oke (1990) provided relative flux calibration; the flux calibrated spectra are presented in Figure 5.

### 3.1. Spectrum of MKN 421

As seen in Figure 5a, the nucleus of MKN 421 is dominated by nonthermal emission with very weak absorption features. This new spectrum is similar to other observations of the nucleus of MKN 421 (e.g., Marchã et al. 1996), with the exception that [OI], [NII], and H $\alpha$  emission lines have been detected. While measurement of relative fluxes for the narrow emission features is complicated by the presence of broad H $\alpha$  emission (Figure 6), and by the contamination of H $\alpha$  absorption from the underlying stellar population (see Figure 4b), the [NII] lines are significantly stronger than the narrow H $\alpha$  feature. Large [NII]/H $\alpha$  ratios are not uncommon in AGN, however (e.g., Veilleux & Osterbrock 1987). Both the broad and narrow emission lines appear to be associated only with the nucleus of MKN 421.

In Fig. 6, we plot a fitted continuum model for MKN 421 along with the measured spectrum, in the region near the detected emission lines. Although the continuum model does not account for all of the structure in the spectrum near the emission lines, it does qualitatively indicate the intrinsic width of the broad-line emission, which has a full-width-at-half-maximum (FWHM) of order 80 Å with detectable emission that extends out to nearly twice this value. Interpretation

---

<sup>4</sup>IRAF is distributed by the National Optical Astronomy Observatories.

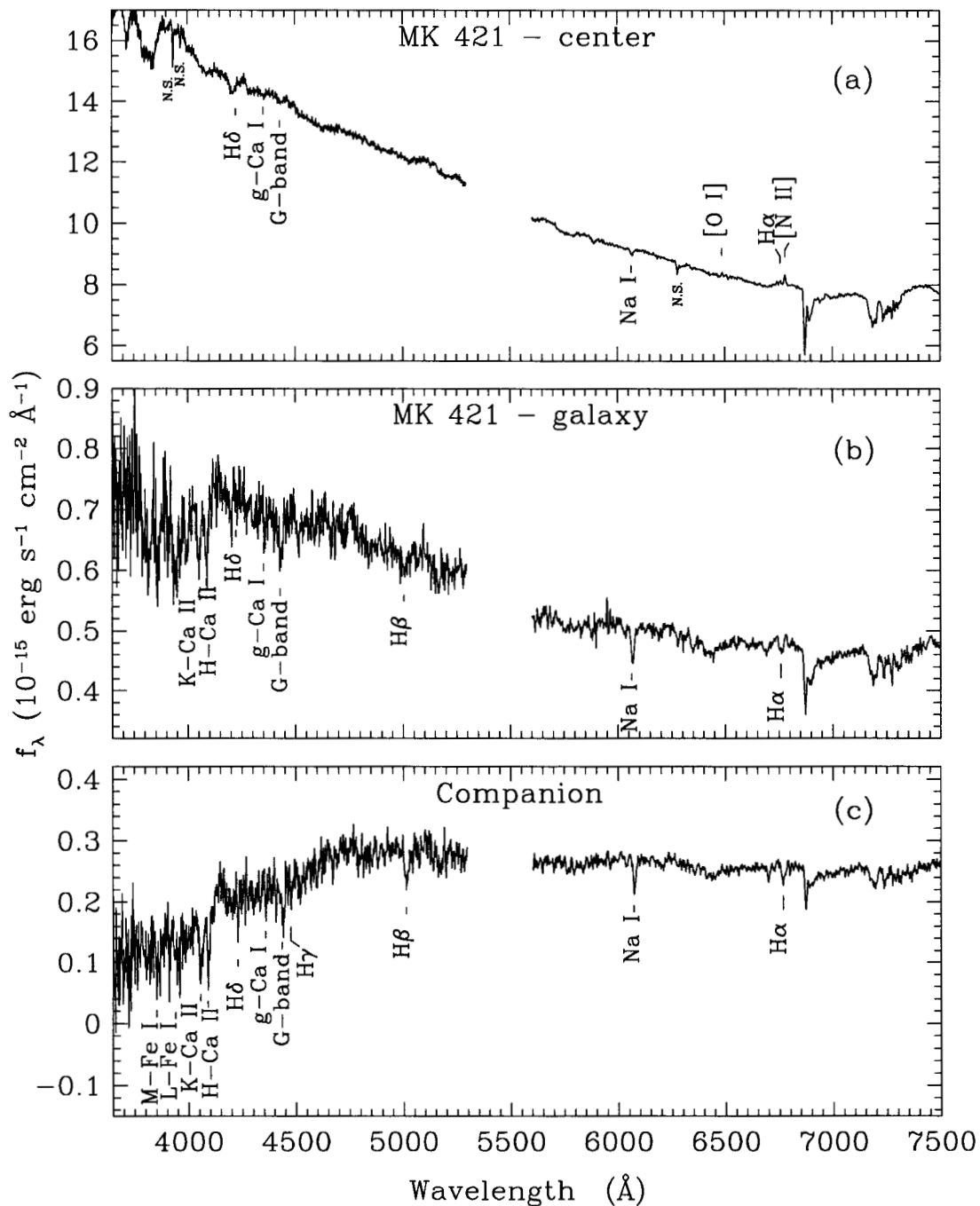


Fig. 5.— Palomar 5 m double spectrograph spectrum of MKN 421 and its companion. The slit was aligned with the two nuclei, and thus covered both galactic bulges as well. (a) MKN 421 shows weak emission at H $\alpha$  and [NII], the first time any emission lines have been noted for this usually almost featureless BL Lac object. (b),(c) MK421 and its companion galaxy have a number of well-defined absorption lines but no detectable emission.

of the width of the broad line emission is complicated by the fact that it is most likely a blend of [NII] and  $H\alpha$ , but even accounting for this the implied velocity dispersion is  $\sim 5000 \text{ km s}^{-1}$ . We discuss some of the implications of this in a later section.

Recently, Morganti et al. (1992) obtained narrow band images roughly centered on the  $H\alpha$  and [NII] lines and reported a total  $H\alpha$ + [NII] flux of  $1.6 \times 10^{-14} \text{ erg s}^{-1} \text{ cm}^{-2}$  for MKN 421. The present observations are the first spectroscopic detection of emission lines associated with the nucleus of MKN 421, confirming this result. The total integrated flux in the broad and narrow emission lines is  $1.7 \times 10^{-14} \text{ erg s}^{-1} \text{ cm}^{-2}$  ( $EW \sim 2.2 \text{ \AA}$ ).

This apparent agreement with Morganti et al. is somewhat misleading, since our estimate includes flux spread over more than  $100 \text{ \AA}$ , while the Morganti et al. estimate was based on a  $50 \text{ \AA}$  FWHM filter which was apparently offset with respect to the centroid of the emission. Thus we actually have detected a significantly *lower* total flux level than Morganti et al., although we cannot quantify the difference. Despite the new detection of emission lines, MKN 421 still falls under the general class of BL Lac objects: the  $4000 \text{ \AA}$  break has a low contrast in the nuclear regions and the derived equivalent widths for the emission lines are significantly less than  $5 \text{ \AA}$ .

The sudden appearance of emission features in previously featureless spectra of BL Lac-type objects is becoming quite common. Just a few years ago, such features were detected in the prototypical BL Lac, BL Lac itself, for the first time (Vermeulen et al. 1995; Corbett et al. 1996). Similar events were discovered in OJ 287 (Sitko & Junkkarinen 1985) and PKS 0521–365 (Ulrich 1981; Scarpa, Falomo, & Pian 1995) as well. The rise and decline of emission-line features in BL Lac-type objects poses an interesting puzzle, and monitoring of these lines should be done as often as possible to determine if their intensity is correlated to that of other bands.

### 3.2. Spectrum of the Host Galaxy

A spectrum of the underlying host galaxy was obtained by averaging spectra on either side of the nucleus (Figure 5b). As found in other spectroscopic observations of the host galaxy (e.g., Ulrich et al. 1975; Ulrich 1978), the spectrum is dominated by absorption features. In addition to the usual strong absorption features in the blue, the Na I  $\lambda\lambda 5890, 5896$  doublet is remarkably strong throughout the galaxy.

### 3.3. Spectrum of MKN 421-5

Similar to the host galaxy of MKN 421, the spectrum of the companion galaxy is dominated by absorption lines (Figure 5c). However, the presence of strong Balmer absorption features indicates that this system is not dominated only by an old stellar population; rather, it must have had recent star formation activity within the last Gyr or so.

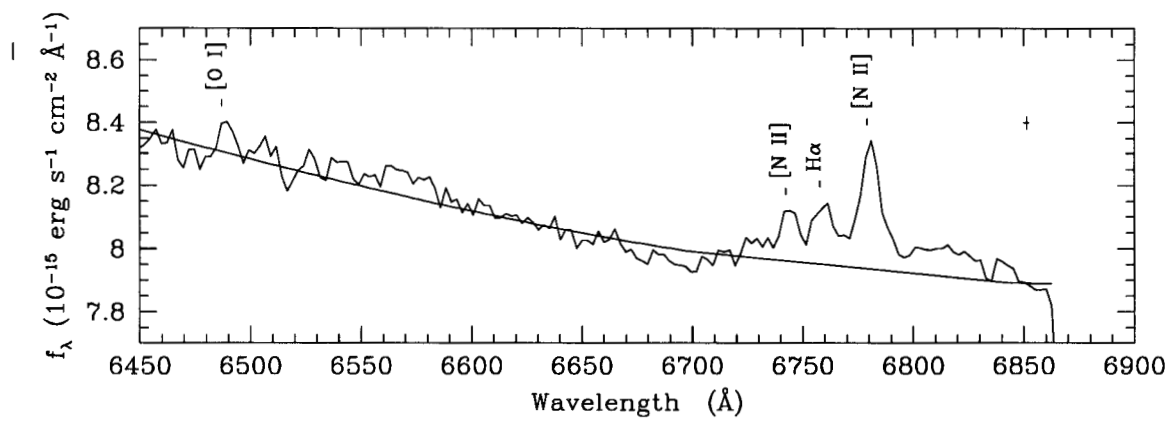


Fig. 6.— Emission lines seen in MKN 421. The curve shows a fitted continuum model. Both broad and narrow emission line components are evident above the continuum.

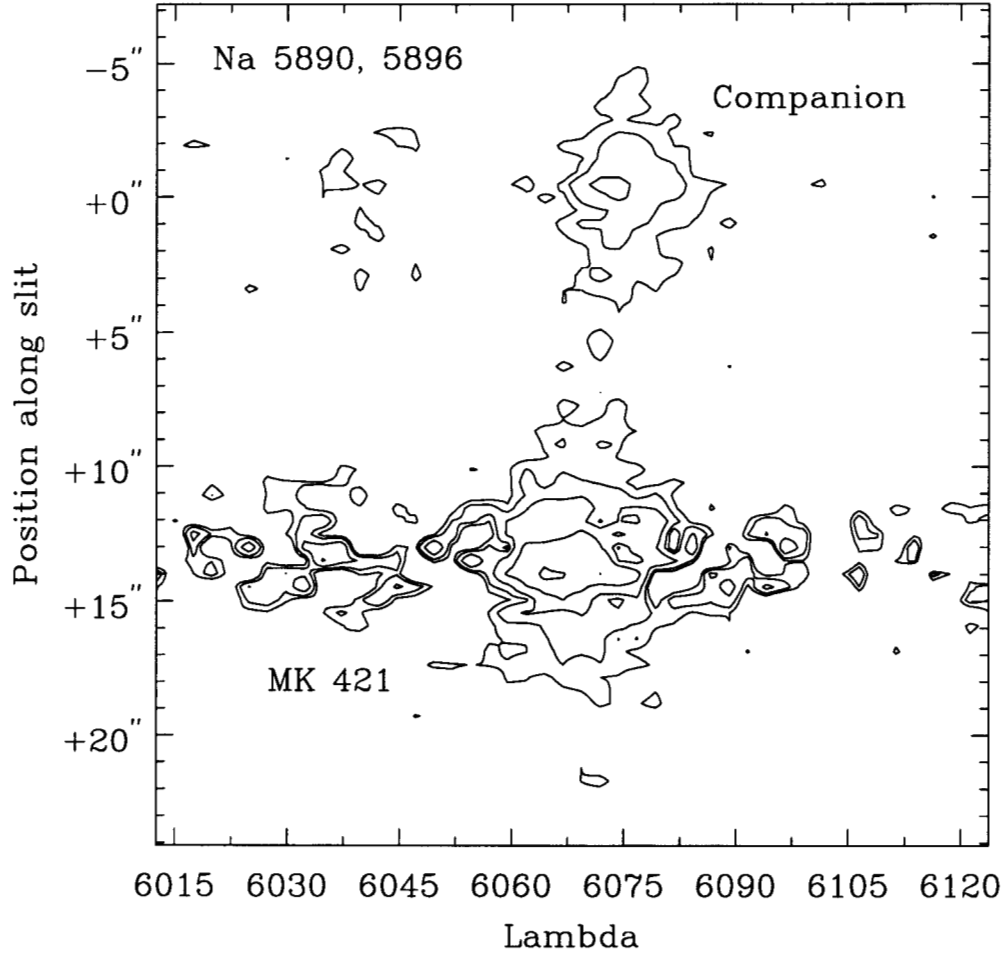


Fig. 7.— Spatially resolved line profile for the NaI doublet. The centroid of the doublet shows a velocity trend that smoothly joins the two galaxies, an indication of a tidal interaction.

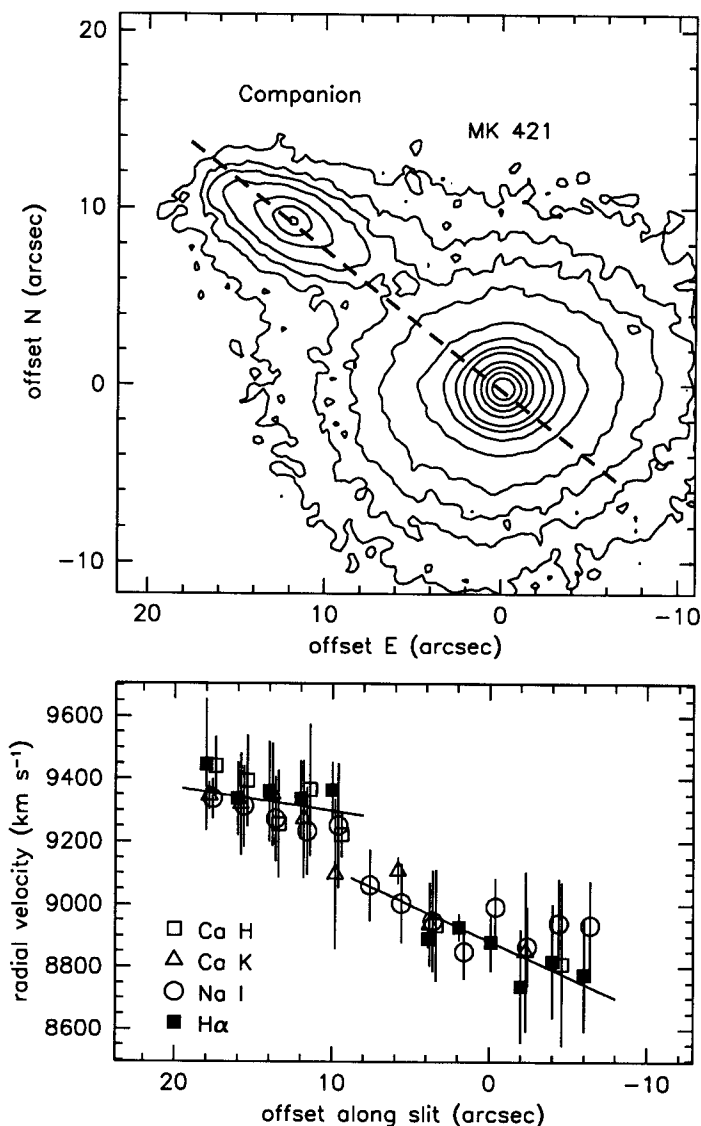


Fig. 8.— (a) Contour plot of Palomar 60'' Gunn r-band image of MKN 421 and companion. The heavy dashed line marks the slit position for the absorption line spectroscopy. (b) Plot of line centroids as a function of slit position. The lines show the fitted velocity gradients across each galaxy separately. The velocity gradient of MKN 421 is consistent with a component of Keplerian rotation that is in the same sense as the companion's velocity relative to MKN 421. The two thus appear to be a bound pair.



The plethora of absorption lines in the optical spectrum permit an accurate redshift determination for this system:  $9380 \pm 50 \text{ km s}^{-1}$ . Ulrich (1978) was one of the first to point out that MKN 421 is part of a large group of galaxies; we now know that radio galaxies tend to form in groups (Zirbel 1997). The close proximity (spatially and in velocity space) of MKN 421 and MKN 421-5 suggest that these two systems may have had significant tidal interactions in the past, and may explain the unusual stellar population of the companion.

### 3.4. Spatially resolved Na absorption

Both MKN 421 and its companion galaxy have high signal-to-noise Na I absorption features which can be used to trace their gas kinematics. A position-wavelength diagram for the two systems is shown in Figure 6. The Na line can be traced almost continuously from MKN 421 to MKN 421-5. The mean velocity as a function of position along the slit for several of the absorption lines is shown in Figure 7. The errors in each individual measurement are quite large given the poor signal-to-noise and the spectral resolution of the observations; nonetheless, the two systems are clearly offset in velocity, but with a sense of velocity continuity between the two galaxies.

Fig. 7 also displays the results of unconstrained least-squares fits for the velocity gradients across each of the two systems. The results of these fits are shown in Table 4. The velocities are not corrected for earth orbital motion; however, the correction for the hour angle of our observation is negligible compared to the errors in the estimates in Table 4.

### 3.5. On limits to radio emission from MKN 421-5

A number of VLA studies of MKN 421 and its immediate vicinity were conducted soon after it was recognized to be a BL Lac object (Ulvestad et al. 1984; 1983); however, the resolution of these studies was not adequate to show the companion due in part to the high dynamic range required (MKN 421 is 0.57 Jy at 20cm). More recent 20cm observations (Laurent-Muhleisen et al. 1993) with higher resolution show complex extended emission in the vicinity of MKN 421, but probably do not have enough dynamic range to detect the companion galaxy nucleus, if its brightness is comparable to the average of its class.

Although there are conspicuous examples of radio-loud Seyferts (primarily Seyfert 1) more typical Seyfert nuclei of both type 1 and 2 emit fluxes of order  $10^{21} \text{ W Hz}^{-1}$  at cm wavelengths (cf. Ulvestad and Wilson 1989 and references therein). At the distance of the companion, this luminosity would produce about 0.5 mJy of 3.5 cm flux density, and of order a factor of 2-3 more than this at 20 cm for a typical Seyfert spectral index of  $-0.5$  to  $-0.7$ . Inspection of a number of VLA maps at various resolutions shows no source of significant strength at the companion galaxy position. However, the complex halo of emission around MKN 421 precludes identifying a source at a level below 1 mJy. Further radio observations should be made to attempt to identify any

compact source associated with the companion galaxy nucleus.

## 4. Discussion

### 4.1. The nature of the companion

The absolute magnitude of the nucleus of MKN 421-5 was given in table 2 as  $M_{F702W} = -16.92$ . It is thus apparently as bright as or brighter than any of the compact nuclear clusters described from HST observations by Phillips et al. (1996) and Carollo et al. (1997), although we are comparing  $V$  band (the HST F555W filter corresponds approximately to Johnson  $V$ ) to approximate  $R$  band results. However, the average values for compact nuclei described in Phillips et al. and Carollo et al. are  $M_V = -12$  to  $-14$  and it is unlikely that large  $V - R$  values would account for more than  $\sim 1$  mag of the difference. A recent detailed HST study of four nearby spirals with compact nuclei (Matthews et al. 1999) gave  $M_B$  values that range from  $-8.5$  to  $-10.4$ , and corresponding  $M_I$  values of  $-9.9$  to  $-11.4$ . This lends more weight to the conclusion that  $V - R$  differences can only account for a small fraction of the brightness difference between MKN 421-5's nucleus and the average of other spiral compact nuclei.

Compact star cluster nuclei are not uncommon among late-type spiral galaxies, although they are often difficult to detect in ground-based images. However, based on the photometric results presented above, the nucleus of MKN 421-5 must be among the most luminous in its class if it comprises an overluminous nuclear cluster.

The alternative is that we are viewing a Seyfert nucleus near the low end of the Seyfert luminosity range. In fact, recent studies have shown that the Seyfert luminosity function extends well below the luminosity of MKN 421-5 (Ho et al. 1996, Ho et al. 1997). It is also worth noting that Malkan et al. (1998), in an HST survey targeting known or potential Seyfert galaxies, found that the presence of a bright, unresolved nucleus in HST images was a nearly perfect indicator of Seyfert activity in a survey of several hundred objects. Thus the lack of emission lines from the nucleus of the companion galaxy is puzzling, given the other indications that the source is non-thermal in nature. However, given the mediocre seeing conditions during the spectroscopic observations, and the extreme compactness of the core, our constraints on emission lines are not yet very restrictive.

The HST results indicate that we are viewing the companion at a substantial inclination relative to its spiral axis. This could contribute to the lack of observed emission lines due to obscuration. If the galaxy is a Seyfert 2, the narrow line emission may in fact be sufficiently diluted by the galactic bulge that it will be difficult to observe from the ground. From the HST image, the nuclear source is probably unresolved; even if we assume its diameter to be  $0.1''$ , the dilution factor under our seeing conditions ( $1.2''$ ) is at least a factor of 10, after accounting for the brightness of the nucleus relative to its surrounding bulge. Clearly, interpretation of

any ground-based observations of this and other similar objects must be tempered with caution because of the danger of these dilution effects.

## 4.2. Implications of the velocity measurements

### 4.2.1. Mass of MKN 421 bulge

As noted above, the shape of the velocity curve is consistent with the behavior expected from tidal interaction. This, combined with the proximity of MKN 421-5 to MKN 421, and the presence of a group of galaxies of similar redshift, leads to the conclusion that MKN 421-5 is undergoing an orbital encounter with MKN 421. Also, since MKN 421-5 is much closer to MKN 421 than any other galaxy in the group, we may treat the pair as a binary system for purpose of estimating the dynamical masses involved.

The statistics of binary galaxies have been treated in detail by Noerdlinger (1975) who showed that the assumption of circular orbits for a binary pair is a conservative one with regard to mass estimation. In fact, the circular orbit approximation is valid up to eccentricities of  $\epsilon \sim 0.4$ , and underestimates the mass by only a factor of 3 in the limit of a parabolic encounter ( $\epsilon = 1$ ).

Thus we estimate a lower limit to MKN 421’s mass  $M$  within the companion’s present projected orbital radius  $R_p$ :

$$M(R_p) \geq \frac{U_r^2 R_p}{G} \quad (1)$$

where  $U_r$  is the companion’s radial velocity and  $G$  is the gravitational constant.

For  $U_r = 496 \text{ km s}^{-1}$  and  $R_p = 10 \text{ Kpc}$  in the comoving frame, the lower limit of the mass is

$$M(R_p) \geq 5.9 \times 10^{11} M_\odot. \quad (2)$$

For moderate ellipticity ( $\epsilon \leq 0.4$ ), Noerdlinger (1975) has shown that the most probable values of the total velocity  $U_T$  and true separation  $R_T$  are likely to be 20-30% higher than the observed values. Thus the most probable value for the bulge mass is about twice the value above, of order  $10^{12} M_\odot$ . Typical giant elliptical rotation curves increase out to radii of order 10 kpc, then flatten and continue out to 50 kpc or more. Since a flat rotation curve implies a linear increase of the dark halo mass with radius, we expect that only of order 10–20% of the total mass of the MKN 421 system is likely to reside within  $R_p$ , the total mass of the galaxy probably approaches  $10^{13} M_\odot$ , among the highest masses of giant elliptical galaxies. Further measurements of the virial velocities of other members of MKN 421’s group should be able to confirm this.

#### 4.2.2. *Mass-to-light ratio*

The CCD photometry of MKN 421 reported by Kikuchi et al. (1987) gives the absolute V magnitude of the MKN 421 host galaxy within a  $13''$  radius of  $M_V(13'') = -21.51 \pm 0.03$ , implying a luminosity of  $3.5 \times 10^{10} M_\odot$ . Note that the emission from other bands, such as radio continuum and X-ray, is almost entirely associated with the AGN rather than the galaxy. Thus, the implied minimum mass-to-light ratio is  $M/L \geq 17$ , indicating a substantial dark matter contribution to the total mass of MKN 421 within  $R_p$ .

This calculation ignores the possible contribution of atomic or molecular gas to the total mass, but no HI has been detected in this system (van Gorkom et al. 1989). IRAS measurements of far-infrared fluxes of MKN 421 (van Gorkom et al.) have been interpreted as due to the presence of a total dust mass of order  $5 \times 10^7 M_\odot$ . If a gas component were present corresponding to this dust level, one might expect up to  $10^9 M_\odot$  of gas in the total galaxy; only a fraction of this would be within  $R_p$ . Thus we expect our derived M/L ratio to be robust.

A number of statistical estimates of the mass-to-light ratios of binary galaxies have yielded values with ranges of 12–32 for pure spiral pairs (Schweizer 1987; Honma 1999) and 22–60 for elliptical pairs (Schweizer 1987). These estimates use galaxies with mean separations of order 60–100 Kpc, and thus include a much greater mass fraction of the whole galaxy than our estimate. As discussed above, typical giant elliptical rotation curves lead one to expect that the total M/L for MKN 421 may be 5–10 times higher than what is measured for this close pair.

#### 4.2.3. *Estimates of MKN 421 central black hole mass*

Wandel (1999), Wandel et al. (1999), Laor (1998) and others have noted the correlation of AGN bulge mass to the mass of a central black hole in cases where a reliable virial mass or reverberation mapping mass could be estimated. Using the curves given in Wandel (1999), and assuming that our estimate of the lower limit to the mass within  $R_p$  is dominated by the bulge mass of MKN 421, we expect a central black hole mass of order  $10^9 M_\odot$ . If this is correct, it would place MKN 421’s central engine among the most massive of black hole candidates.

We can also derive a provisional upper limit to the black hole mass in the following manner. Based on the unsaturated HST image, the nuclear emission falls within a single HST pixel, implying an upper limit to the radius of the optical emission region of  $\leq 15$  pc. If we assume that all of the observed broad line emission in our spectrum originates from this same region, then we get an upper limit to the black hole mass by assuming that the orbiting material that produces the largest observed broad-line velocity is at the largest allowed radius, and again using equation (1) above. By this approach, we find

$$M_{BH} \leq 2.2 \times 10^{10} M_\odot. \quad (3)$$

We can also use the parametric relations given by Laor (1998) and Wandel et al. (1999) to make an independent estimate of the size of the broad-line region (BLR) based on the AGN bolometric luminosity. Wandel et al. give a black hole mass estimate based on the size of the BLR and  $\Delta v_{FWHM}$ , the FWHM of the measured broad-line velocity dispersion:

$$M_{BH} \approx 1.45 \times 10^5 M_{\odot} \left( \frac{c\tau_{BLR}}{1 \text{ light day}} \right) \left( \frac{\Delta v_{FWHM}}{1000 \text{ km s}^{-1}} \right)^2. \quad (4)$$

The size of the BLR can be estimated from (Kaspi et al. 1997; Wandel et al. 1999):

$$r_{BLR} = 15 L_{44}^{1/2} \text{ light days}. \quad (5)$$

where  $L_{44}$  is the bolometric luminosity. For MKN 421, estimates of the bolometric luminosity over the 0.1 to 1  $\mu\text{m}$  band vary considerably, and it is unclear whether the quiescent or high-state luminosity is more appropriate. Using a bolometric luminosity derived from our HST magnitudes and the conversion given in Laor (1998), we find  $L_{44} \sim 120$ , which gives  $r_{BLR} = 164$  light days. A further uncertainty arises from the line-blending in our observed broad-line emission. If we assume that one species (probably  $H\alpha$ ) is dominant in forming the broad line emission, then we use  $\Delta v_{FWHM} \approx 3300 \text{ km s}^{-1}$  from our spectrum above. The implied black hole mass is then  $M_{BH} \sim 2.5 \times 10^8 M_{\odot}$  which is of the same order of magnitude as the estimate from the bulge mass above.

A black hole mass of  $10^9 M_{\odot}$  is of order 0.25% of the total dynamical mass out to 10 Kpc. Thus it is not in itself enough to affect the large scale dynamics between the two galaxies, although it would certainly strongly influence the inner bulge regions. It is notable that the center of mass of the system will likely be significantly displaced from the position of the black hole, perhaps by a few hundred pc or more, depending on the companion mass and the dark matter distribution. Careful measurements of the virial motion of the stars near the center of MKN 421 may be able to detect such an offset, which would provide independent confirmation of the proximity of MKN 421-5 to MKN 421.

#### 4.2.4. The dynamical state of the system

The smooth rise in the rotation curve of MKN 421 out to  $R_p$  is consistent with expectations for a post-encounter system, in which any major velocity distortions produced by the encounter have relaxed and bulk tidal motions now dominate. However we can not rule out the possibility that this is the companion's first approach toward MKN 421. It is also possible that there are distortions in the velocity curves that are unresolved at our present sensitivity. Since we cannot unambiguously infer the companion's true velocity from radial velocity measurements alone, we cannot prove that the system is bound, and we can only base our estimates of the tidal effects on the global properties we observe. Despite these caveats, there are a number of different lines of evidence that point to a bound and tidally relaxed system.

An obvious, though not compelling, piece of evidence is the fact that we observe the companion galaxy this close to MKN 421 at all, at the relatively late epoch of the system. The probability that we are observing first encounter between two high-ranking cluster galaxies cannot be estimated based on this single case alone. However, based on the galaxy count of Ulrich (1978) and on our own Palomar images over a 12 arcmin field around Mkn 421, there are potentially 7 to 10 galaxies of comparable brightness to MKN 421-5, in a volume of order  $6 \times 10^{16} \text{pc}^3$ , of order  $10^4$  times the volume containing MKN 421 and its companion. Since MKN 421 will probably tend to significantly perturb the local potential, the chance of near encounters with it are not determined simply by random; however, we estimate that the chance observation of such an encounter is of order 1% or less for any snapshot of similar clusters.

If the system is not in the initial phase of a first encounter, it follows that (a) it is likely to be bound (due to the mass dominance of MKN 421 and the narrow range of phase space required for MK421-5 to have the required escape velocity); and (b) that it is tidally relaxed, since the relaxation time for the system as observed is in the range of 100 Myr, relatively short compared to the time of cluster formation.

The apparent lack of significant dust in the companion, and its overall morphology also support the case for a post-encounter system. Comparing MKN 421-5 with the atlas of HST Seyfert images given in Malkan et al. (1998) we find that MKN 421-5 shows similarities to a number of spirals, most notably to MKN 176, which is at a similar redshift and apparent inclination. However, MKN 421-5 is conspicuous for its lack of dust features compared to all of the galaxies in Malkan et al., including MKN 176 and other galaxies of similar morphology and redshift. During close galaxy encounters, tidal interactions are expected to sweep out dust and gas, either expelling it into tidal tails or causing infall of the gas into the galaxy cores.

Another relevant observation is the evidence presented above for fairly recent star-formation in the companion galaxy. Recent simulations of hierarchical galaxy encounters (cf. Bekki 1999 & references therein) have shown that star forming activity in the satellite galaxy is a likely result of such an interaction. A number of recent HST studies have found a significant number of companions near QSO host galaxies (Bahcall et al. 1995; Disney et al. 1995) which appear to be undergoing some type of interaction with the QSO host. Canalizo and Stockton (1997) found that at least one companion galaxy in such a system (PG 1700+518) showed evidence of a relatively young stellar population.

What is perhaps surprising in the case of MKN 421 and MKN 421-5 is that, although simulations such as those of Bekki (1999) indicate that the companion galaxy is likely to evolve to a dwarf elliptical or irregular as a result of the encounter, MKN 421-5 appears to in fact be a relatively normal spiral, without any apparent major disruption or irregularity. This system thus presents a challenge to models which cannot account for preservation of such structure even in what was probably a strong tidal encounter between these two systems. It is notable that MKN 421-5, as a probable Seyfert, is likely to have a massive compact object in its nucleus. The presence of a large central mass may in fact have important dynamical consequences in stabilizing

a satellite galaxy in such an encounter.

#### 4.2.5. *A schematic geometry for the system*

To postulate a possible three-dimensional geometry for this pair of galaxies, we combine a number of related pieces of evidence that bear on the geometry, including our measured velocity curves, the apparent inclination of the companion spiral, the major and minor axes of MKN 421, and parameters associated with the central mass of MKN 421, although the latter are included mainly for comparison rather than as constraints on the global geometry.

The position angle of the center of the companion relative to MKN 421 is  $53^\circ$ , and we estimate that the projected major axis of the spiral lies at a position angle of  $65^\circ$ . Thus the projected rotation axis (perpendicular to the major axis of the spiral) of MKN 421-5 is at a position angle of  $335^\circ$ . The inclination of the spiral is more difficult to estimate, since the shape may be confused by an inner bar feature not easily distinguished in the images. However, it appears that the spiral inclination is in the range of  $45^\circ$  to  $60^\circ$  to the line-of-sight.

If we assume that the disk of the spiral and the orbital plane are roughly coincident (this is reasonable if the systems are tidally relaxed), then we can make a first order schematic estimate of the overall geometry of the system, if the two galaxies are bound in an orbit of only moderate ellipticity. This schematic view of the system is depicted graphically in Figure 8. We have not attempted to quantify this geometry further; we present it simply as a qualitative baseline which can be refined (or revised) by future observations.

VLBI observations of the inner one-sided radio jet of MKN 421, combined with other considerations have led to the suggestion that we are viewing MKN 421’s jet at an angle of  $\leq 34^\circ$  from the axis. More recent VLBI imagery and estimates of the jet doppler factors from both VLBI and gamma-ray observations (Piner et al. (1999); Gaidos et al. 1996) indicate more conclusively that the jet angle must be  $\leq 5^\circ$  with respect to the observation vector. The projected position angle of the inner jet from VLBI observations is  $\sim 320^\circ$ . We have plotted this position angle in Fig. 8 for comparison. For the case of a small angle with respect to the line-of-sight, the approximate coincidence of the projected position angle with that of the spiral axis and the possible orbital plane is presumably an accident. However, if the jet is actually physically aligned with the other angular momentum vectors in the system, then a much larger angle for it with respect to the line-of-sight is favored.

An outstanding question in MKN 421 and in BL Lac objects in general is how well-aligned the jet axis is with the line-of-sight to the AGN. If the results based on estimates of the doppler factors are correct, and the jet axis is inclined by  $\leq 5^\circ$ , then we are led to conclude that either the orbital plane of the two galaxies are not well-aligned with the perpendicular to the jet axis, or plane of the spiral companion is not well-aligned with the overall orbital plane. In either case the residual torques may have observable consequences, either in precession effects or tidal velocity

Table 4: Fitted velocities and velocity gradients for MKN 421 & companion.

Source	$\bar{v}$ km s <sup>-1</sup>	$\sigma_v$ km s <sup>-1</sup>	$\nabla v$ km s <sup>-1</sup> as <sup>-1</sup>	$\sigma_{\nabla v}$ km s <sup>-1</sup> as <sup>-1</sup>
MKN 421	8884	27	23.0	6.0
MKN 421-5	9380	50	7.4	4.0

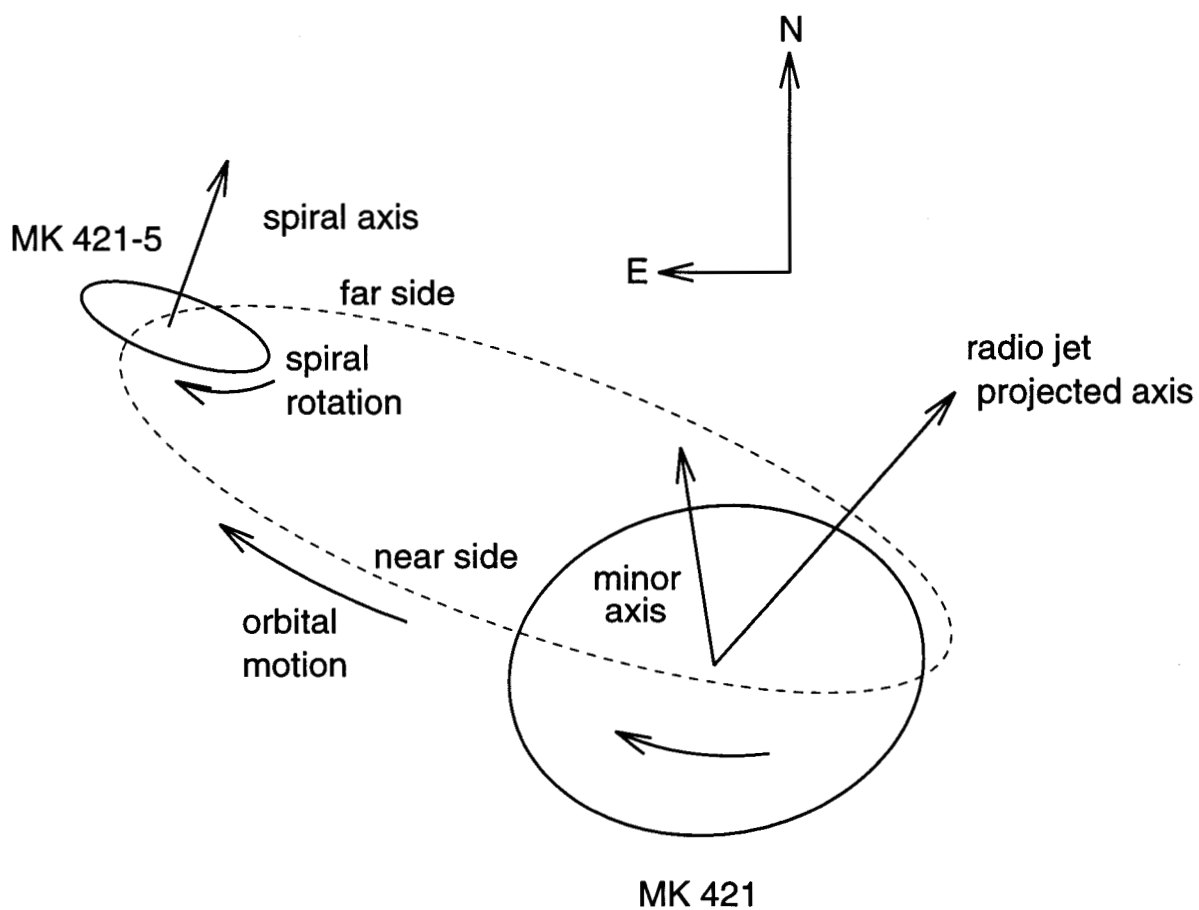


Fig. 9.— A suggested schematic geometry for the MKN 421 + companion system.



distortions of the system. More complete velocity mapping may provide information on the latter consequence. As to the former effect, further analysis is necessary to estimate whether there might be observable effects, since the precession time scale would be expected to be long compared to the orbital time scale.

Studies of alignment of radio jets and rotation axes of Seyfert galaxies have shown that there is very little correlation between the two (Schmitt et al. 1997), and that there is in fact a paucity of systems with alignment closer than about  $10^\circ$ . Similar studies of alignment of AGN jet axes with the orbital axes of elliptical hosts is complicated by the difficulty of estimating the rotation axes of elliptical galaxies. In the present case, we observe a rotation curve for MKN 421 which extends out to approximately  $\pm 200 \text{ km s}^{-1}$ . If this is the projected radial velocity from a dominant component in the rotation around an axis which is  $\leq 5^\circ$ , the true space velocity of the rotation would extend out to  $\pm 2300 \text{ km s}^{-1}$ . This value appears to high to be plausible for this system and is inconsistent with the value derived for the companion galaxy unless its orbital plane is also nearly face-on.

#### 4.2.6. *Companion rotation: Prograde or Retrograde?*

We conclude this section by briefly discussing the sense of the companion rotation. The rotation curve shown in Fig. 7 shows that the eastern end of MKN 421-5 is redshifted relative to the western end which is closest to MKN 421. This indicates a rotation which is clockwise on the sky, and corresponds to a prograde rotation relative to the projected rotation of the bulge of MKN 421.

This feature of the system may be important to the stability of the companion. Future simulations should look in more detail at the effects of retrograde vs. prograde rotation in a tidal encounter.

## 5. Conclusions

We have gathered evidence that supports the following conclusions:

1. MKN 421’s nearest companion galaxy MKN 421-5 appears to be an early-type spiral, rather than elliptical. It also appears to have a notable lack of dust compared to similar galaxies. We conclude that this feature is consistent with a system which has undergone some level of tidal stripping from its encounter with MKN 421. Spectral evidence suggests moderately recent star-formation activity in the companion, a feature which is known to accompany galaxy interactions.
2. MKN 421-5 contains a Seyfert-like nucleus, but without detectable emission lines in ground-based spectroscopy. We find that its luminosity is probably too high for a compact

nuclear star cluster and conclude it is most likely to be an AGN, in spite of the lack of spectroscopic evidence.

3. We confirm the published radial velocity for MKN 421-5. We find that MKN 421-5 is very likely to be bound to MKN 421, and its orbital velocity is consistent with the trend in the bulk rotational velocity of MKN 421, suggesting tidal interaction. We do not see any evidence for large scale tidal distortion of either MKN 421 or MKN 421-5, and suggest that the system is tidally relaxed.
4. We report the first spectroscopic observation of emission lines from MKN 421's nucleus, notably  $H\alpha$  and NII. Both broad and narrow components of  $H\alpha$  are present, with the broad line emission showing a velocity dispersion of several thousand  $\text{km s}^{-1}$ , typical of QSO emission lines. Spectroscopic monitoring of these lines should continue.
5. The observed orbital velocity of the companion MKN 421-5 provides a lower limit on the mass of MKN 421's bulge of  $5.9 \times 10^{11}$  solar masses, with an estimated bulge mass-to-light ratio of  $\geq 17$ . This value is at the high end of the range for giant elliptical galaxies. If MKN 421 contains a black hole as the central engine, its bulge mass may imply a black hole mass of order  $10^9 M_{\odot}$ , and arguments based on the spectroscopic evidence support this.

We thank R. Linfield and the staff of Palomar Observatory for their invaluable help with the observations, and Glenn Piner for his helpful comments on the manuscript. This work was performed at the Jet Propulsion Laboratory, California Institute of Technology, under contract with the National Aeronautics and Space Administration. The National Radio Astronomy Observatory is a facility of the National Science Foundation, operated under a cooperative agreement by Associated Universities Inc. This research is based in part on observations made with the NASA/ESA Hubble Space Telescope, obtained from the data archive at the Space Telescope Science Institute. STScI is operated by the Association of Universities for Research in Astronomy, Inc. under NASA contract NAS 5-26555.

## REFERENCES

- Buckley et al. 1996 ApJ Letters 472,9.
- Comastri, A. F. et al. 1997, ApJ 480, 534.
- Corbett, E. A., Robinson, A., Axon, D. J., Hough, J. H., Jeffries, R. D., Thurston, M. R., & Young, S. 1996, MNRAS, 281, 737
- Falomo, R., 1996, MNRAS 283, 241.
- Gaidos, J. et al. 1996, Nature 383, 319.

- Heidt, J. 1999, in Takalo L. O., and Sillanpaa, A. (eds.), *Proc. BL Lac Phenomena*, PASP159, 367.
- Hernquist, L., and Mihos, J. C., 1995, *ApJ* 448, 41.
- Hickson, P., Fahlman, G. G., Auman, J. R., Walker, G. A. H., Menon, T. K., and Ninkov, Z., 1982, *ApJ* 258, 53.
- Honma, M., 1999, LANL preprint astro-ph 9904079.
- Kikuchi, S., and Mikami, Y., 1987, *ApJ* 39, 237.
- Knapp, G.R., Bies, W.I., and van Gorkom, J. H., 1990 *AJ*99, 476.
- Liu, F. K., et al. 1997, *A&A Suppl.* 123, 569.
- Loar, A., 1998 *ApJ*505, L83.
- Mukherjee, R., et al., 1997, *ApJ* 490, 116.
- Marchã, M. J. M., Browne, I. W. A., Impey, C. D., & Smith, P. S. 1996, *MNRAS*, 281, 425
- Morganti, R., Ulrich, M.-H., & Tadhunter, C. N. 1992, *MNRAS*, 254, 546
- Oke, J. B. 1990, *AJ*, 99, 1621
- Piner, B. G., Unwin, S. C., Wehrle, A. E., Edwards, P. G., Fey, A. L., and Kingham, K. A., 1999, *ApJ*, in press.
- Scarpa, R., Falomo, R., & Pian, E. 1995, *A&A*, 303, 730
- Schmitt, H. R., Kinney, A. M., Storchi-Bergmann, T., and Antonucci, R., 1997 *ApJ*477, 623.
- Schweizer, L.Y., 1987 *ApJS*64, 427.
- Sitko, M. L., & Junkkarinen, V. T. 1985, *PASP*, 97, 1158
- Shlosman, I., Begelman, M. C., Frank, J., 1990 *Nature* 345, 679.
- Simien, F., and Prugniel, Ph., 1997, 122, 521; also 126, 15, 519.
- Simien, F., and Prugniel, Ph., 1998, 131, 287.
- Tosti, G., Fiorucci, M., Luciani, M. et al. 1998 *A&A*339, 41.
- Ulrich, M.-H. 1978, *ApJ*, 222, L3
- Ulrich, M.-H. 1981, *A&A*, 103, L1
- Ulrich, M.-H., Kinman, T. D., Lynds, C. R., Rieke, G. J., & Ekers, R. D. 1975, *ApJ*, 198, 261
- Ulvestad, J.S, and Wilson, A. S., 1989, *ApJ*343, 659.

- van Gorkom, J.H., Knapp, G. R., Ekers, R.D., et al., 1989 AJ97, 708.
- Veilleux, S., & Osterbrock, D. E. 1987, ApJS, 63, 295
- Vermeulen, R. C., Ogle, P. M., Tran, H. D., Browne, W. A., Cohen, M. H., Readhead, A. C. S., & Taylor, G. B. 1995, ApJ, L5
- Wandel, A., 1999, LANL preprint astro-ph 9904370.
- Wandel, A., Peterson, B., and Malkan, M., 1999, ApJ(in press), (LANL preprint astro-ph 9905224).
- Zirbel, E. L. 1997, ApJ, 476, 489
- Zhang, F. J., and Baath, L. B., 1990, A&A236, 47.